Analysis of the running-in phase of a passively safe thorium breeder pebble bed reactor

Wols, FJ; Kloosterman, JL; Lathouwers, D; van der Hagen, THJJ

DOI
10.1016/j.anucene.2015.02.043

Publication date
2015

Document Version
Final published version

Published in
Annals of Nuclear Energy

Analysis of the running-in phase of a passively safe thorium breeder pebble bed reactor

Wols, Frank; Kloosterman, Jan-Leen; Lathouwers, Danny; van der Hagen, Tim

DOI
10.1016/j.anucene.2015.02.043

Publication date
2015

Document Version
Final published version

Published in
Annals of Nuclear Energy

Annals of Nuclear Energy 81 (2015) 227–239

Contents lists available at ScienceDirect

Annals of Nuclear Energy

journal homepage: www.elsevier.com/locate/anucene

Analysis of the running-in phase of a Passively Safe Thorium Breeder Pebble Bed Reactor

F.J. Wols *, J.L. Kloosterman, D. Lathouwers, T.H.J.J. van der Hagen

Delft University of Technology, Department of Radiation Science and Technology, Mekelweg 15, 2629JB Delft, The Netherlands

ARTICLE INFO

Article history:
Received 23 October 2014
Received in revised form 24 February 2015
Accepted 26 February 2015
Available online 18 March 2015

Keywords:
Running-in phase
Pebble Bed Reactor
Thorium breeder
Passive safety

ABSTRACT

The present work investigates the running-in phase of a 100 MW_{th} Passively Safe Thorium Breeder Pebble Bed Reactor (PBR), a conceptual design introduced in previous equilibrium core design studies by the authors. Since U-233 is not available in nature, an alternative fuel, e.g. U-235/U-238, is required to start such a reactor. This work investigates how long it takes to converge to the equilibrium core composition and to achieve a net production of U-233, and how this can be accelerated.

For this purpose, a fast and flexible calculation scheme was developed to analyze these aspects of the running-in phase. Depletion equations with an axial fuel movement term are solved in MATLAB for the most relevant actinides (Th-232, Pa-233, U-233, U-234, U-235, U-236 and U-238) and the fission products are lumped into a fission product pair. A finite difference discretization is used for the axial coordinate in combination with an implicit Euler time discretization scheme.

Results show that a time dependent adjustment scheme for the enrichment (in case of U-235/U-238 start-up fuel) or U-233 weight fraction of the feed driver fuel helps to restrict excess reactivity, to improve the fuel economy and to achieve a net production of U-233 faster. After using U-235/U-238 start-up fuel for 1300 days, the system starts to work as a breeder, i.e. the U-233 (and Pa-233) extraction rate exceeds the U-233 feed rate, within 7 years after start of reactor operation.

The final part of the work presents a basic safety analysis, which shows that the thorium PBR fulfills the same passive safety requirements as the equilibrium core during every stage of the running-in phase. The maximum fuel temperature during a Depressurized Loss of Forced Cooling (DLOFC) with scram remains below 1400 °C throughout the running-in phase, quite a bit below the TRISO failure temperature of 1600 °C. The uniform reactivity coefficients of cores with U-235/U-238 driver fuel are much stronger negative compared to U-233/Th driver fuel, which implies that the stronger reactivity insertion by water ingress and the reactivity addition by xenon decay during a DLOFC without scram can be compensated without fuel temperatures exceeding 1600 °C.

1. Introduction

The running-in phase of a 100 MW_{th} Passively Safe Thorium Breeder Pebble Bed Reactor (PBR) is investigated in the present work. The conceptual design of such a reactor was introduced in a previous work by the authors (Wols et al., 2015). The design combines inherent safety, a high outlet temperature, reduced lifetime of the radiotoxic waste and an enlarged resource availability. However, a high fuel pebble handling speed and fuel reprocessing rate is required. During previous design studies by the authors (Wols et al., 2015) the equilibrium core composition was determined.

However, U-233 is not available in nature, so the start-up of a thorium breeder PBR requires another fuel. Low enriched uranium will be considered as a start-up fuel in this work, but plutonium (and minor actinides) may also provide an alternative, its use has already been considered previously in combination with thorium inside PBRs (Rütten and Haas, 2000; Chang et al., 2006; Mulder et al., 2010). The build-up of certain relevant actinides, e.g. U-234, U-235 and U-236, may take quite some time. Therefore, it is important to determine from which moment the reactor starts breeding, i.e. a net production of U-233, and how much time it takes to converge to the equilibrium core composition.

In addition to answering these questions, the running-in phase strategy should also be chosen carefully in order to minimize the additional U-235 fuel consumption, achieve equilibrium quickly and to maintain a critical core configuration, while restricting the amount of excess reactivity, at any time. In order to achieve this, the fresh fueled core composition and the enrichment of the U-235/U-238 feed fuel during the initial start-up phase and the

* Corresponding author. Tel.: +31 152784041.
E-mail address: f.j.wols@tudelft.nl (F.J. Wols).

http://dx.doi.org/10.1016/j.anucene.2015.02.043
0306-4549/

U-233 weight fraction of the driver fuel in the remainder of the running-in phase should be chosen carefully over time.

Finally, the thorium PBR should also be passively safe during the whole running-in phase. For this purpose, a basic safety analysis, i.e. calculation of the uniform reactivity coefficient, maximum power density, maximum fuel temperature during a Depressurized Loss of Forced Cooling (DLOFC) with scram and the maximum reactivity insertion due to water ingress, is performed at different moments of the chosen running-in phase strategy.

The most common code in literature for modeling the running-in phase of multi-pass PBRs is VSOP (Very Superior Old Programs) which was developed in Germany during the high temperature reactor program (Rütten et al., 2010). The VSOP code calculates the core depletion over the whole start-up phase until the equilibrium core, and was used for instance to model the running-phase of the HTR-10 (Xia et al., 2011). Furthermore, NRG's PANTHERMIX code is also capable of modeling the start-up phase of a PBR (Oppe et al., 2001; Marmier et al., 2013).

The calculation scheme previously applied by Wols et al. (2015) for the design of the reactor only provides the option to calculate the equilibrium core composition directly. This code scheme could be extended to a full time dependent version, but the calculations would become very time consuming. The scheme also does not offer enough flexibility to vary the relevant fuel management parameters over time. In this scheme, a burnup calculation is performed and afterwards the fuel concentrations are shifted to a new lower grid position.

For this work, a new calculation scheme was developed to perform the running-in phase calculations. This scheme solves the depletion equations in MATLAB for only the most relevant actinides (Th-232, Pa-233, U-233, U-234, U-235, U-236 and U-238), while the fission products are lumped into a single fission product pair. Furthermore, several simplifications were made in the cross section generation scheme to reduce the computation time. The depletion equations are solved including an axial fuel movement term, so fuel movement and depletion are accounted for simultaneously, increasing the flexibility of the model. A finite difference discretization is used for the height term and an implicit Euler scheme to solve the time dependent term. With this scheme, any of the relevant parameters can easily be varied over time.

A detailed description of the scheme and the simplifications used is given in Section 3, while Section 4 demonstrates that the influence of the simplifications in the depletion equations and the cross section generation scheme is fairly small ($\approx 0.3\%$) for the conversion ratio (CR) of the equilibrium core configuration. Though the ratio between the fissile atom production and consumption rate may deviate a bit more during the running-in phase itself, this will not influence the trends observed during the present work as the time-scales involved remain similar. Despite the simplifications used to reduce the computation time, the new running-in phase model provides a very useful and flexible tool to analyze and optimize the running-in phase strategy and to gain insight into the time-scales involved in the running-in phase.

The next section gives a more detailed introduction of the 100 MW_{th} Passively Safe Thorium Breeder Pebble Bed Reactor (PBR), followed by a description of the running-in phase model, calculation of the equilibrium core with the new model, results of the running-in phase calculations, a basic safety analysis of the thorium PBR during the running-in phase and conclusions and recommendations.

2. The thorium PBR equilibrium core design

The cylindrical core of the 100 MW_{th} Passively Safe Thorium Breeder Pebble Bed Reactor (PBR) consists of a central driver zone surrounded by a breeder zone. The driver zone has a 100 cm radius with a soft neutron spectrum for enhanced fission. The breeder zone of 200 cm thickness has a harder neutron spectrum to enhance conversion. The difference in spectra between the two zones is achieved by a difference in the metal loading per pebble. 30 g thorium, in the form of ThO_2, is loaded per breeder pebble and 3 g HM (10 w% U-233) per driver pebble. Breeder pebbles make two passes within 1000 days, while the driver pebbles are recycled four times in slightly more than 80 days to obtain a critical core configuration. It is assumed that the uranium content of the breeder and driver pebbles can, and will, be reprocessed after their final passage. The system's mass balance shows a higher extraction rate of U-233 (and Pa-233) than the insertion rate for the equilibrium core. A more detailed description of the equilibrium core calculation scheme is given by Wols et al. (2014a, 2015).

Furthermore, the system was also shown to combine breeding with passive safety, as fuel temperatures were shown to remain below 1600 °C during a DLOFC without scram and water ingress only causes a relatively small reactivity increase (+1497 pcm), which can be compensated by the temperature feedback only (Wols et al., 2015). An overview of the relevant fuel and core design parameters of the 100 MW_{th} passively safe thorium breeder PBR (Wols et al., 2015) is given in Table 1.

2.1. Geometry of the neutronics model

A schematic view of the reactor geometry used by the authors during past and current neutronic studies (Wols et al., 2014a, 2015) is shown in Fig. 1. The geometry is based upon the HTR-PM design (Zheng and Shi, 2008; Zheng et al., 2009). Porous side reflector regions model the presence of helium in the control rod and coolant channels. Pure helium regions, e.g. the top plenum, are homogenized with adjacent graphite regions to avoid neutronically thin media in the diffusion calculations. A density of 1.76 g/cm^3 is used for the graphite reflector material and 1.55 g/cm^3 for the carbon brick.

3. Running-in phase model

First, the calculational model for the running-in phase is discussed in Section 3.1, followed by a discussion of the cross section

Table 1
Core and fuel design parameters of the 100 MW_{th} thorium breeder PBR design.

Core design parameters	
Power	100 MW_{th}
Core radius	300 cm
Driver zone radius	100 cm
Core height	1100 cm
Pebble packing fraction	0.61
Driver/breed z. passes	4/2
Total res. time breeder	1000 d
Total res. time driver	80.38 d
$^{233}U_{in-out}$	+8.58 g/d
$^{233}Pa_{in-out}$	−8.91 g/d
Fuel design parameters	
Fuel mass breeder pebble	30 g HM
Fuel mass driver pebble	3 g HM
U-233 fraction of driver fuel	10 w%
Pebble radius	3.0 cm
Fuel kernel radius	0.25 mm
Fuel zone radius	2.5 cm
Material	**Thickness (mm)**
Porous Carbon buffer layer	0.09
Inner Pyrocarbon layer	0.04
Silicon Carbide layer	0.035
Outer Pyrocarbon layer	0.035

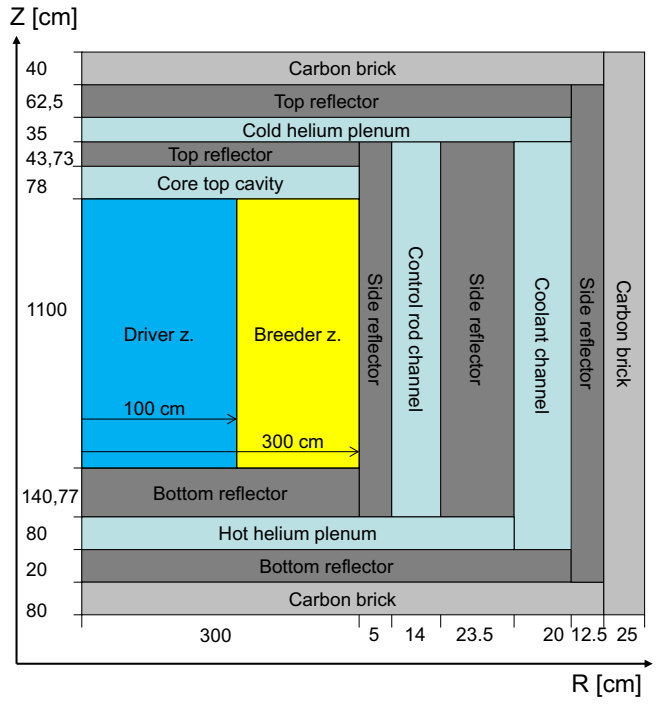

Fig. 1. Schematic view of the thorium breeder PBR geometry used in the neutronics calculations. The geometry is based upon the HTR-PM (Zheng and Shi, 2008).

preparation method in Section 3.2, which also includes a discussion of a time-invariant version of the model to calculate the equilibrium core directly.

3.1. Time-dependent fuel depletion model

Assuming that the fuel moves only in the axial direction, the generalized burnup equation (Massimo, 1976) of a nuclide k, with concentration N_k, is given by:

$$\frac{\partial N_k}{\partial t} + v_z \frac{\partial N_k}{\partial z} = \phi \sum_{i=l}^{m} N_i \sigma_{fi} y_{ik} + \phi \sum_{s=r}^{q} N_s \sigma_{as} y_{sk} + \sum_{j=n}^{p} N_j \lambda_j \alpha_{jk} - \lambda_k N_k - \phi N_k \sigma_{ak} \quad (1)$$

Here, v_z is the axial pebble velocity, ϕ the neutron flux, σ_{fi} is the microscopic fission cross section of isotope i and σ_{as} is the microscopic absorption cross section of isotope s, λ_j and λ_k are the decay constants of isotopes j and k, y_{ik} is the yield of isotope k due to fission in isotope i and y_{sk} is the yield of isotope k due to absorption in isotope s, while α_{jk} is the probability that isotope k is formed after decay of isotope j.

A simplified time dependent core depletion model was developed for parametric studies of the running-in phase by numerically solving the burnup equations for the important actinides (i.e. Th-232, Pa-233 and the uranium isotopes), while the fission products are modeled by a single fission product pair for computational ease. Isotopes beyond uranium, e.g. plutonium, are neglected in the scheme as the build up of these isotopes was found to be negligible, in terms of conversion ratio and criticality, for the equilibrium core configuration considered in the previous work of the authors (Wols et al., 2015). The mass ratio of Pu-238 over U-233 was only a factor $3 \cdot 10^{-12}$ for the extracted breeder pebbles and $8 \cdot 10^{-5}$ for the driver pebbles, still a rather small fraction.

The burnup equations will be solved as a function of height, using finite differences, and time, using an implicit Euler discretization scheme, for both driver and breeder zone. So, a single radially averaged concentration is obtained for each zone, in conjunction with the more extensive equilibrium core calculation scheme previously developed by the authors (Wols et al., 2014a, 2015).

The advantage of the new model is that it allows for relatively fast calculations over the whole length of the running-in phase, while the code is flexible in varying several interesting time dependent parameters, such as the enrichment of the feed fuel, pebble recycling speeds, reactor power and initial core loading. The influence of these parameters on the progress of the running-in phase, i.e. k_{eff} over time, length of the running-in phase, U-233 mass inside and outside the core, can be evaluated with the model. Though possible, variations of the total driver pebble residence time and the reactor power over time are not considered in the present work. Such variations are less desirable from an operational perspective and they were found unnecessary to achieve the goals of this work.

Due to the simplifications of the lumped fission product pair and not considering the build-up of actinides beyond uranium it is not possible to do waste characterization studies, but this is also not the goal of the model.

3.1.1. Start-up driver fuel

Since U-233 is not available in nature, an alternative has to be considered as a driver fuel for the start-up phase of the reactor. The most logical candidate and the one considered in this work is enriched uranium, but plutonium (and minor actinides) might also be considered. During this initial start-up phase, the burnup equations of U-235, U-238 and fission product pair, FP5, will be solved for the driver zone. This initial phase is referred to as the '*U-235 fueled phase*' in the remainder of this work.

It is assumed that the uranium content from the discarded enriched uranium driver pebbles will not be reprocessed, or at least that this uranium will not be mixed with the U-233 produced in the breeder pebbles. Therefore, the U-236 concentration is not considered as it takes a long time to reach a significant concentration, i.e. this will happen only with continuous reprocessing of U-233 later on. U-237 is also not considered since it has a very short half-life (6.75 days). In the later stage of the running-in phase, after switching to U-233 as a driver fuel the build-up of U-236 will be taken into consideration.

The burnup equations for U-235, U-238 and the lumped fission product pair (denoted by FP5, neglecting fast fission in U-238) are then given by:

$$\frac{\partial N_{U5}(z,t,p)}{\partial t} + v_z(t) \frac{\partial N_{U5}(z,t,p)}{\partial z} = -N_{U5}(z,t,p) \sigma_{a,U5} \phi(z,t) \quad (2)$$

$$\frac{\partial N_{U8}(z,t,p)}{\partial t} + v_z(t) \frac{\partial N_{U8}(z,t,p)}{\partial z} = -N_{U8}(z,t,p) \sigma_{a,U8} \phi(z,t) \quad (3)$$

$$\frac{\partial N_{FP5}(z,t,p)}{\partial t} + v_z(t) \frac{\partial N_{FP5}(z,t,p)}{\partial z} = N_{U5}(z,t,p) \sigma_{f,U5} \phi(z,t) - N_{FP5}(z,t,p) \sigma_{a,FP} \phi(z,t) \quad (4)$$

Here z refers to the axial position in the core, being 0 at the top and H at the bottom, t refers to the time and there is the pebble class p, which accounts for the actual passage number of the pebble. For all passages p, the initial condition of isotope x is given by:

$$N_x(z,0,p) = N_{fresh,x}(z), \quad (5)$$

while the boundary condition is:

$$N_x(0,t,p) = N_{feed,x}(t) \quad (p=1), \quad (6)$$

$$N_x(0,t,p) = N_x(H,t,p-1) \quad (p>1). \quad (7)$$

So, the concentration at the top of the core is given by the feed fuel for the first passage or the concentration at the bottom of the core in the previous passage. $N_{fresh,FP5}$ and $N_{feed,FP5}$ are obviously zero.

The balance equations are discretized using finite differences for the z-coordinate and implicit Euler for the time variable. Time is denoted with index i, and k is used to index the axial coordinate. For U-235 and U-238, denoted by x, this results in:

$$\frac{N_{x,k}^{i+1}-N_{x,k}^{i}}{\Delta t}+v_z^{i+1}\frac{N_{x,k}^{i+1}-N_{x,k-1}^{i+1}}{\Delta z}=-N_{x,k}^{i+1}\sigma_{a,x}\phi_k^{i+1} \tag{8}$$

Which after collecting of terms results in:

$$N_{x,k}^{i+1}\left(\Delta z+\sigma_{a,x}\phi_k^{i+1}\Delta z\Delta t+v_z^{i+1}\Delta t\right)-v_z^{i+1}\Delta t N_{x,k-1}^{i+1}=N_{x,k}^{i}\Delta z \tag{9}$$

The resulting matrix–vector system ($\mathbf{A}N^{i+1}=N^{i}\Delta z$) is solved consecutively for each pebble passage p by MATLAB. Only the diagonal and lower diagonal elements of the matrix $\mathbf{A}$ are non-zero. For the fission product pair concentration (FP5) the discretization is similar, except for an additional production term, $N_{U5,k}^{i+1}\sigma_{f,U5}\phi_k^{i+1}\Delta z\Delta t$, appearing in the right hand side of the equation. The fission product pair concentration can be solved by MATLAB, after solving for the U-235 concentration.

3.1.2. Thorium, U-233

After a while, a sufficient amount of U-233 has been produced to start using it for the driver fuel without ever supplying additional U-235/U-238 fuel afterwards. This will be referred to as the '*U-233 fueled phase*' in the remainder of this work. The breeder zone is fed with thorium pebbles directly from the start of reactor operation. For both the breeder zone and the U-233 fueled phase of the driver zone, the nuclide balance equations of Th-232, Pa-233 (assuming instantaneous decay of Th-233), U-233 till U-236 and the fission product pair concentrations, denoted by FP3, have to be solved. The nuclide balance equations for these nuclides are given in the following:

$$\frac{\partial N_{T2}(z,t,p)}{\partial t}+v_z(t)\frac{\partial N_{T2}(z,t,p)}{\partial z}=-N_{T2}(z,t,p)\sigma_{a,T2}\phi(z,t) \tag{10}$$

$$\frac{\partial N_{P3}(z,t,p)}{\partial t}+v_z(t)\frac{\partial N_{P3}(z,t,p)}{\partial z}=-N_{P3}(z,t,p)[\sigma_{a,P3}\phi(z,t)+\lambda_{P3}]+N_{T2}(z,t,p)\sigma_{c,T2}\phi(z,t) \tag{11}$$

$$\frac{\partial N_{U3}(z,t,p)}{\partial t}+v_z(t)\frac{\partial N_{U3}(z,t,p)}{\partial z}=-N_{U3}(z,t,p)\sigma_{a,U3}\phi(z,t)+\lambda_{P3}N_{P3}(z,t,p) \tag{12}$$

$$\frac{\partial N_{U4}(z,t,p)}{\partial t}+v_z(t)\frac{\partial N_{U4}(z,t,p)}{\partial z}=-N_{U4}(z,t,p)\sigma_{a,U4}\phi(z,t)+N_{U3}(z,t,p)\sigma_{c,U3}\phi(z,t) \tag{13}$$

$$\frac{\partial N_{U5}(z,t,p)}{\partial t}+v_z(t)\frac{\partial N_{U5}(z,t,p)}{\partial z}=-N_{U5}(z,t,p)\sigma_{a,U5}\phi(z,t)+N_{U4}(z,t,p)\sigma_{c,U4}\phi(z,t) \tag{14}$$

$$\frac{\partial N_{U6}(z,t,p)}{\partial t}+v_z(t)\frac{\partial N_{U6}(z,t,p)}{\partial z}=-N_{U6}(z,t,p)\sigma_{a,U6}\phi(z,t)+N_{U5}(z,t,p)\sigma_{c,U5}\phi(z,t) \tag{15}$$

$$\frac{\partial N_{FP3}(z,t,p)}{\partial t}+v_z(t)\frac{\partial N_{FP3}(z,t,p)}{\partial z}=-N_{FP3}(z,t,p)\sigma_{a,FP}\phi(z,t)+N_{U3}(z,t,p)\sigma_{f,U3}\phi(z,t) \tag{16}$$

These equations are solved by a similar matrix–vector system as for the U-235, U-238 and fission product pair concentrations in the previous subsection.

3.1.3. Time-steps and updating the neutron flux

A time-step size, Δt, of 2.5 h is used to solve the system of equations during the calculations in this work. In Section 5, an 80.4 days total driver pebble residence time and 4 driver pebble passes are used, so it would take 4.4 h to traverse a single grid cell of 10 cm height. So, a 2.5 h time-step is used to obtain sufficiently accurate results.

The neutron flux $\phi(z,t)$ is obtained for both driver and breeder zone by performing a k_{eff} calculation of the core with DALTON, an inhouse developed neutron diffusion solver. The magnitude of the flux vector $\phi(z,t)$ is scaled to the desired power production during each time-step Δt, while the expensive update of the neutron flux by DALTON is performed only after multiple steps Δt. At the start of the U-235 fueled phase, the flux is updated by DALTON during every $5\Delta t$ steps. If the relative change in k_{eff} and the neutron flux shape becomes smaller than 0.02%, the flux update interval is doubled, but the flux is updated at least every 1000 time-steps Δt. At the start of the U-233 fueled phase, the flux update interval is reset again to every $5\Delta t$ steps, because significant changes in flux shape and k_{eff} can be anticipated again.

3.1.4. Uranium and protactinium stockpiles

After each calculation step, the uranium (so U-233 till U-236) extracted from the breeder zone during the initial U-235 fueled phase and the uranium extracted from both breeder and driver zone during the U-233 fueled phase are added into a uranium stockpile. The Pa-233 content of the extracted pebbles is added to a protactinium stockpile. A schematic view of the use of the uranium and protactinium stockpiles in the different stages of the running-in phase is given in Fig. 2. It is assumed that reprocessing, i.e. the separation of uranium and protactinium, takes place instantaneously and that the uranium content in the stockpile is perfectly mixed. Obviously, in practice there would be some delay in the reprocessing and there will be multiple stockpiles, because a critical mass of U-233 should be avoided. These stockpiles will have a somewhat different composition depending on the extraction date of the uranium, which specifies the buildup of U-234 till U-236 that has taken place. Though such effects are relevant for more detailed fuel management studies in advanced stages of reactor design, they are not expected to have a significant influence on the trends observed during the more general studies in the present work.

In the U-233 fueled phase, the concentrations of U-234, U-235 and U-236 in the driver fuel fed to the core, i.e. $N_{U4}(z=0,t,p=1), N_{U5}(z=0,t,p=1)$ and $N_{U6}(z=0,t,p=1)$, are based on their mass ratio's in the uranium stockpile. Obviously, the masses of the uranium isotopes inserted during the U-233 fueled phase are subtracted from the uranium stockpile.

After each time-step of the calculation, the amount of Pa-233 decayed in the stockpile is transferred to the U-233 stockpile. In reality, a longer timer interval before extracting the decayed U-233 from the protactinium stockpile may be more practical, but this won't affect the results significantly as the total amount of U-233 in both stockpiles remains the same.

3.2. Cross sections

Obviously, the accuracy of the results obtained by the numerical scheme strongly depends on the reliability of the cross section data, i.e. the cross sections and neutron flux $\phi(z,t)$, used by the model. So, the cross sections should be collapsed with a neutron spectrum representative of the true operating conditions of the driver and the breeder zone. Microscopic cross sections have been determined using the average nuclide concentrations (and temperature) of the driver and the breeder zone in an equilibrium core configuration calculation, which is discussed in more detail in the following. This way, cross sections only have to be generated for a single core slab using the CSAS and XSDRN modules included in SCALE6 (ORNL, 2009), instead of at multiple heights. Furthermore, it only has to be performed for the equilibrium core calculations and not during the

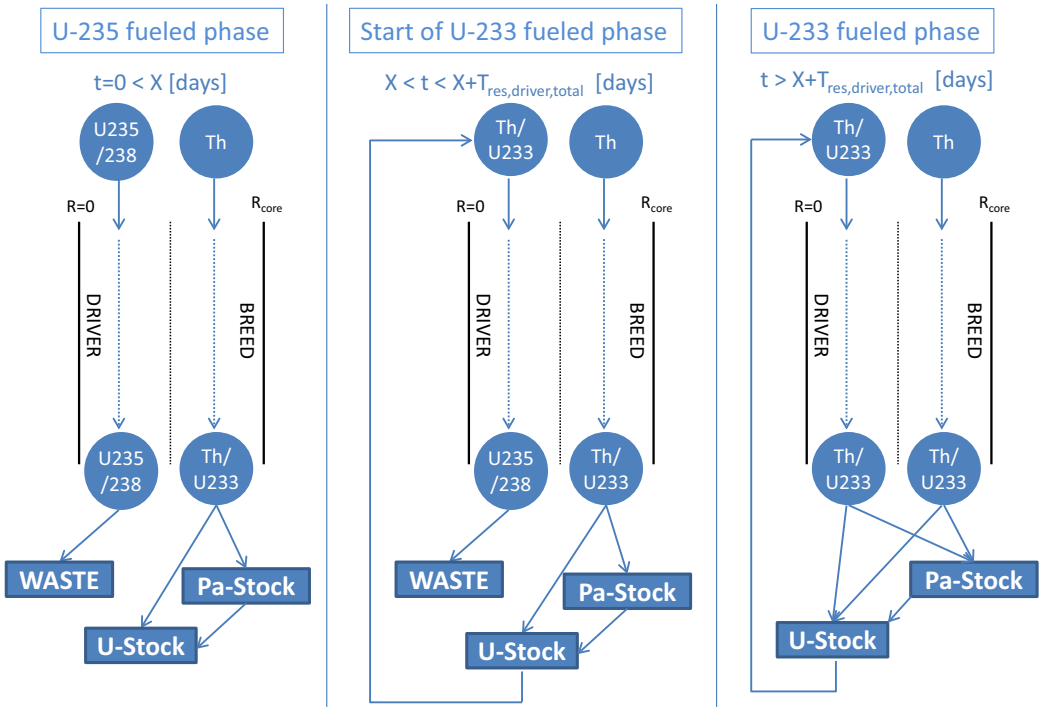

Fig. 2. Schematic view of the use of the uranium and protactinium stockpile, after the final pebble passage, during the U-235 fueled phase and during, the start and remainder of, the U-233 fueled phase. *X* refers to the moment the U-233 fueled phase is started.

time dependent calculation of the running-in phase. The influence of these approximations will be demonstrated to be fairly small for the equilibrium core configuration in Section 4. During the running-in phase, the ratio between fissile atom production and consumption may deviate somewhat more as the core composition deviates further from the equilibrium core, but this does not have a significant impact upon the time-scales involved and the trends observed in the present work. To ensure the accuracy of the model, the cross sections are collapsed to five energy groups and the nuclide balance equations are solved using these five group cross sections and the five group fluxes obtained by DALTON, i.e. the reaction rates are determined by summing over five groups: $\sigma\phi(z,t) = \sum_{g=1}^{5}\sigma_g\phi_g(z,t)$.

A 2-D(r,z) macroscopic cross section set, to be used by DALTON, is generated by adding the microscopic cross sections multiplied with the nuclide concentrations obtained at the different heights of the driver and breeder zone using the ICE-module of SCALE6. Obviously, the macroscopic cross sections of the graphite and TRISO coating layers in the pebbles, and surrounding helium, as well as the graphite in the reflector regions are also included in the 2-D cross section set.

3.2.1. Equilibrium core calculation scheme and cross sections

By setting the $\frac{\partial N_x(z,t)}{\partial t}$-terms in the previous section to zero, it is possible to calculate the equilibrium core composition by solving a similar matrix–vector system, but then without the implicit Euler time discretization. The flux of the equilibrium core is not known a priori, so an initial guess has to be made. The nuclide balance equations are solved using this flux guess and a new DALTON calculation is performed afterwards. This process is repeated until convergence is reached. However, the average nuclide concentrations of Th-232, Pa-233 and the uranium isotopes also require an initial guess. So, using the updated average nuclide concentrations, the microscopic cross sections can be updated and the equilibrium composition is calculated again. After a few cross section updates, this process has also converged and the equilibrium core is determined as well as the cross section set for the time dependent calculation of the running-in phase. The U-235 and U-238 cross sections used in the driver zone during the U-235 fueled phase are collapsed after a 1D radial XSDRN-calculation using representative nuclide concentrations for the state of the reactor during this initial phase.

The equilibrium core composition obtained in previous work by Wols et al. (2015), with all relevant fission products included by ORIGEN, was used to determine the ratio between the different energy groups in $\sigma_{a,FP}$. The absolute value of $\sigma_{a,FP}$ was adjusted to approximate a critical core, i.e. $k_{eff} = 1.00086$, for the same operating conditions, e.g. a driver pebble residence time of 80.38 days, as the equilibrium core previously calculated (Wols et al., 2015). The fission product pair absorption cross sections used are shown in Table 2.

4. Equilibrium core results

The equilibrium core composition of the thorium PBR design, discussed in Section 2, was calculated with the time-invariant version of the newly developed scheme, as discussed in Section 3.2.1. This was done for three reasons. Firstly, the equilibrium core result of the new scheme will be used as a reference for the reactor configuration at the end of the running-in phase in order to analyze if, and how rapidly, the equilibrium core is approximated. Secondly,

Table 2
The five group fission product pair cross section.

Group	Energy range	$\sigma_{a,FP}$ [b]
1	0.9–20 MeV	0.034
2	30 eV–0.9 MeV	2.158
3	0.625–30 eV	33.36
4	0.15–0.625 eV	60.14
5	10 meV–0.15 eV	490.0

the microscopic cross section set obtained for the equilibrium core composition will be used for the driver fuel, during the U-233 fueled phase, and for the breeder zone throughout the whole running-in phase calculation, as explained in Section 3.2. Thirdly, a comparison between the equilibrium core composition, calculated with the new simplified scheme (Section 3.2.1) and the original equilibrium core calculation scheme (Wols et al., 2015), gives a proper estimate of the error introduced by the simplifications in the new running-in phase scheme.

A total driver pebble residence time of 80.38 days was used, as this was the result of the original equilibrium core calculation scheme. The mass flow rates calculated by the original equilibrium core calculation scheme and the new simplified method are shown in Table 3.

The mass flow rates calculated by the different code schemes show a close agreement. The system is predicted to be a breeder by both codes, though the system's net balance of U-233, including Pa-233, is slightly more negative for the new scheme, −0.66 g/d compared to −0.33 g/d. Though this may be a large difference in relative terms, this deviation of 0.33 g/d is quite small in absolute terms considering that a bit more than 100 g of uranium is fissioned in the system per day. For the purposes of this work, this deviation is acceptable. Furthermore, the fraction of the power produced in the driver zone deviates only 0.2% between the two codes.

5. Analysis of the running-in phase

This section presents results of some initial running-in phase studies, followed by a separate analysis of the U-235 fueled phase and the U-233 fueled phase in Sections 5.2 and 5.3. The k_{eff} values that will be shown in this section are of interest from a fuel management perspective, so the influence of control rods is neglected in this analysis. Obviously, a value of k_{eff} above unity in this work does not imply that the reactor will work in a supercritical state in reality. So, ideally a k_{eff} of at least unity is desirable in this analysis. On the other hand, large amounts of excess reactivity should also be avoided from a fuel economy perspective.

5.1. Initial studies of the running-in phase

First, results of some initial running-in phase studies will be presented for different feed fuel enrichments during the U-235 fueled phase. A uniform fresh driver fuel composition of 11 w% U-235 and 89 w% U-238 was used yielding an initial k_{eff} of 1.0075 for the fresh start-up core. For the feed driver fuel, three enrichments were investigated during the initial U-235 fueled phase, being 12 w%, 13 w% and 14 w% U-235. After 2000 days, the U-233 fueled phase starts and 10 w% U-233 fueled driver pebbles are added to the core, in consistence with the equilibrium core configuration (see Table 1). The k_{eff} is shown on two time-scales for the different enrichments during the U-235 fueled phase in Fig. 3a and b, while Fig. 3c shows the U-233 mass in the uranium stockpile over a time interval of 50 years, and Fig. 3d shows the U-234, U-235 and U-236 fraction in the uranium stockpile over a time interval of 200 years.

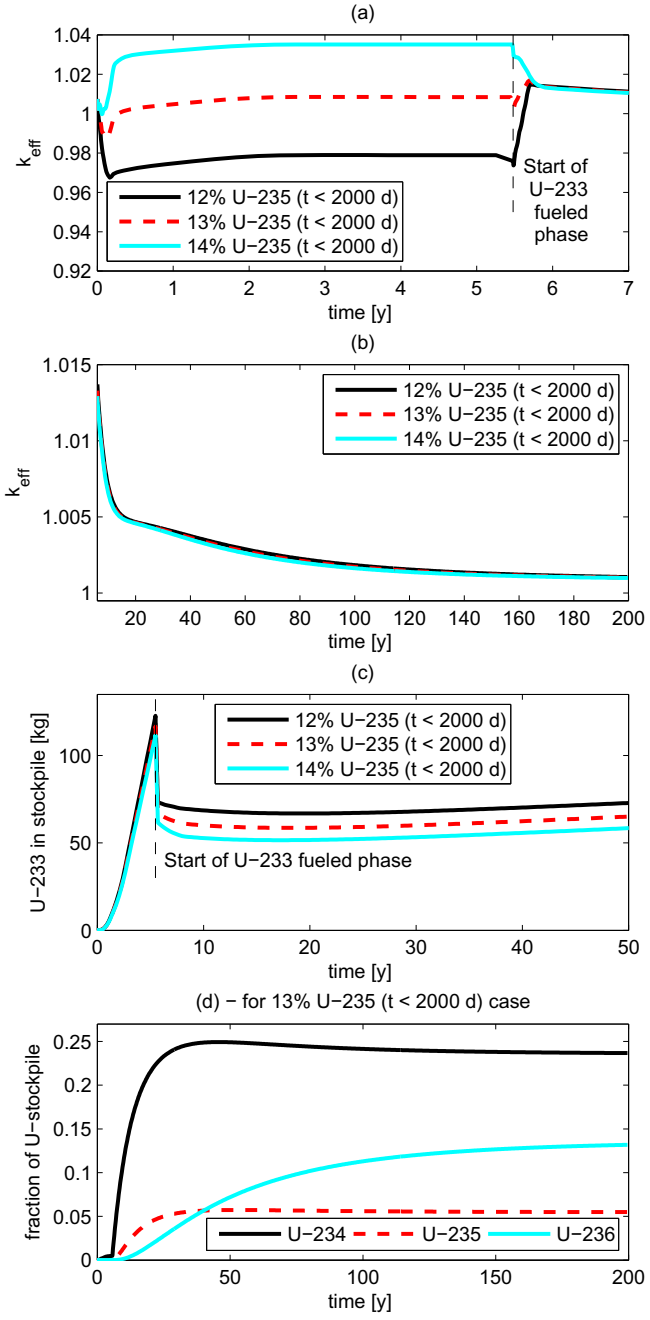

Fig. 3. k_{eff} over short (a) and longer time-scale (b) and U-233 stockpile over time (c) using different U-235 enrichments during the initial U-235 fueled phase of 2000 days. The U-234, U-235 and U-236 fraction in the uranium stockpile are shown over time for a 13% U-235 feed fuel enrichment (d).

Fig. 3a shows that the k_{eff} remains below unity over the whole U-235 fueled phase with a 12% enrichment during the U-235 fueled phase. For a 13% enrichment, k_{eff} is smaller than unity in the initial part of the U-235 fueled phase, but becomes larger than unity after 103 days and achieves a maximum value of 1.0085 in the U-235 fueled phase. For a 14% enrichment, the k_{eff} is generally larger than unity during the U-235 fueled phase, but it is 0.9998 for a very short moment. The maximum k_{eff} during the U-235 fueled

Table 3
Comparison between equilibrium core results using the new and the original calculation scheme.

	Original equilibrium scheme	Running-in phase scheme
$T^{total}_{res,driver}$	80.38 d	80.38 d
$^{233}U_{in,driver}$	695.65 g/d	695.65 g/d
$^{233}U_{out,driver}$	605.81 g/d	605.61 g/d
$^{233}U_{out,breed}$	81.25 g/d	81.34 g/d
$^{233}Pa_{out,driver}$	7.68 g/d	7.88 g/d
$^{233}Pa_{out,breed}$	1.23 g/d	1.48 g/d
$^{233}U_{in-out}$	+8.58 g/d	+8.69 g/d
$^{233}Pa_{in-out}$	−8.91 g/d	−9.35 g/d
Net $^{233}U_{in-out}$	−0.33 g/d	−0.66 g/d
Power–Driver z.	95.67 MW_{th}	95.45 MW_{th}

phase is 1.0352, which is a lot higher than required. So, from a first view, an enrichment somewhat above 14% is required for the very initial stage ($t < 100$ days) of the U-235 fueled phase and a 13% enrichment afterwards. After starting the U-233 fueled phase, the k_{eff} rapidly approaches a similar value for the three different cases, because the same driver fuel is fed to the core for the three cases in the U-233 fueled phase.

For the long term behavior (Fig. 3b) it can be seen that k_{eff} remains above unity during the U-233 fueled phase. For all three cases, the k_{eff} drops quite rapidly, i.e. within 15 years, to a k_{eff} of 1.005 and than more gradually decreases to a value around 1.001, closely approximating the k_{eff} of 1.00086 in the equilibrium configuration.

Fig. 3c shows that the U-233 mass in the stockpile increases rapidly in the U-235 fueled phase, since none of the U-233 extracted from the breeder zone is fed back to the core. After the start of the U-233 fueled phase, the amount of U-233 in the stockpile drops rapidly by approximately 50 kg, because U-233 is fed to the driver zone and not yet extracted, as shown in the middle scheme of Fig. 2. After the first U-233/Th driver fuel pebbles are extracted from the core, the amount of U-233 in the stockpile only reduces very slowly. Later on, the U-233 mass in the stockpile increases again after a net production of U-233 is achieved. It can also be seen that the build up of U-233 in the stockpile is a bit lower if the U-235 enrichment increases during the U-235 fueled phase. This is because a lower flux is needed to yield the same power production, which leads to a reduction of the neutron capture rate in Th-232, and because a larger fraction of the power is produced in the driver zone.

Fig. 3d shows that the U-234, U-235 and especially U-236 fractions in the uranium stockpile take quite some time to reach equilibrium, which is still not fully achieved after 200 years, so multiple reactor lifetimes. However, one can also notice from Fig. 3c that the minimum U-233 mass in the stockpile, after the start of the U-233 fueled phase, is quite a bit above zero. Firstly, this is undesirable from a fuel economy perspective. Secondly, the U-234, U-235 and U-236 concentrations extracted from the core are somewhat diluted after they are added to the uranium stockpile, which somewhat slows down reaching an equilibrium.

The start of the U-233 fueled phase should be timed in such a way that a sufficient amount of U-233 has been produced to feed the core without ever supplying additional U-235/U-238 fuel afterwards, while avoiding a significant excess amount of U-233. Therefore, the starting moment of the U-233 fueled phase was varied between 1300, 1500 and 2000 days in the following simulations. A 13% enrichment is used during the U-235 fueled phase, as this led to a k_{eff} close to one over the largest part of the U-235 fueled phase, as shown in Fig. 3a. By shortening the length of the U-235 fueled phase, the excess of U-233 in the stockpile can be reduced, a net U-233 production may be achieved earlier and the U-234, U-235 and U-236 concentrations may approach equilibrium faster. Again, the k_{eff} is shown on a short and longer time-scale in Fig. 4a and b.

For practical application, the enrichment should be increased a bit during the first 100 days of the U-235 fueled phase to ensure a k_{eff} larger than unity over the whole 200 years (Figs. 3a and 4a), which will be investigated in the next section. More importantly, an earlier start of the U-233 fueled phase (1300 days) leads to a smaller uranium stockpile (Fig. 4c) and consequently the U-234, U-235 and U-236 fractions also reach equilibrium values a lot faster (Fig. 4d). Fig. 4b shows that this also influences k_{eff}, which seems to approach an equilibrium much faster if the U-233 fueled driver pebbles are added after 1300 days.

The top graph of Fig. 5 shows the system's net U-233 mass flow balance, i.e. inflow minus outflow, over time for a 1300 days U-235 fueled phase. The net balance becomes negative after 9.16 years

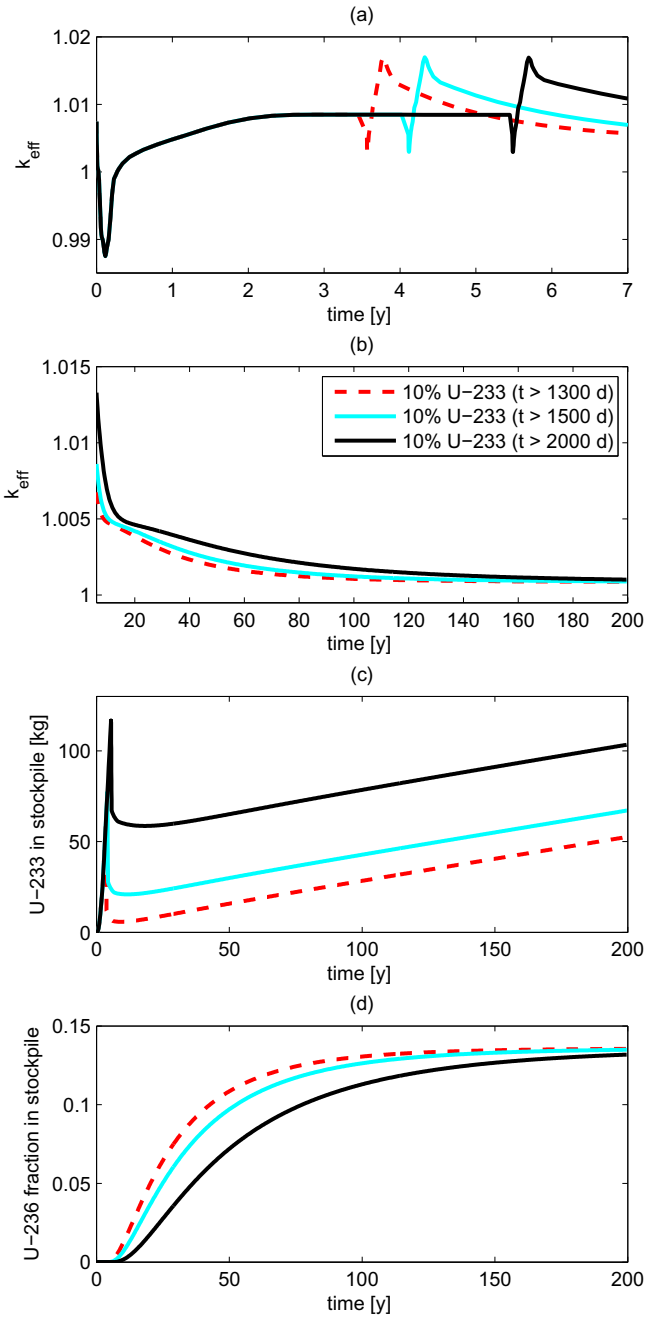

Fig. 4. k_{eff} over short (a) and longer time-scale (b), the U-233 stockpile over time (c) and the U-236 fraction in the uranium stockpile over time (d) using different starting moments for the U-233 fueled phase. A 13% enrichment was used during the U-235 fueled phase.

and the system operates as a breeder. The U-233 net mass flow balance reaches an equilibrium after 200 years. The net U-233 mass flow balance, including Pa-233, of the equilibrium core (−0.6604 g/d) is closely approximated at the end of the simulation (−0.6619 g/d), as well as k_{eff} being only 1.7 pcm lower for the equilibrium core.

The lower graph of Fig. 5 shows the U-234, U-235 and U-236 fractions in the uranium stockpile. The U-234 and U-235 fractions reach maxima after 25.6 and 29.3 years, followed by a slight decrease of their fraction, almost stabilizing after 200 years. The U-236 fraction slowly increases and is still slightly increasing after 200 years, but this does not have a significant influence on k_{eff} anymore.

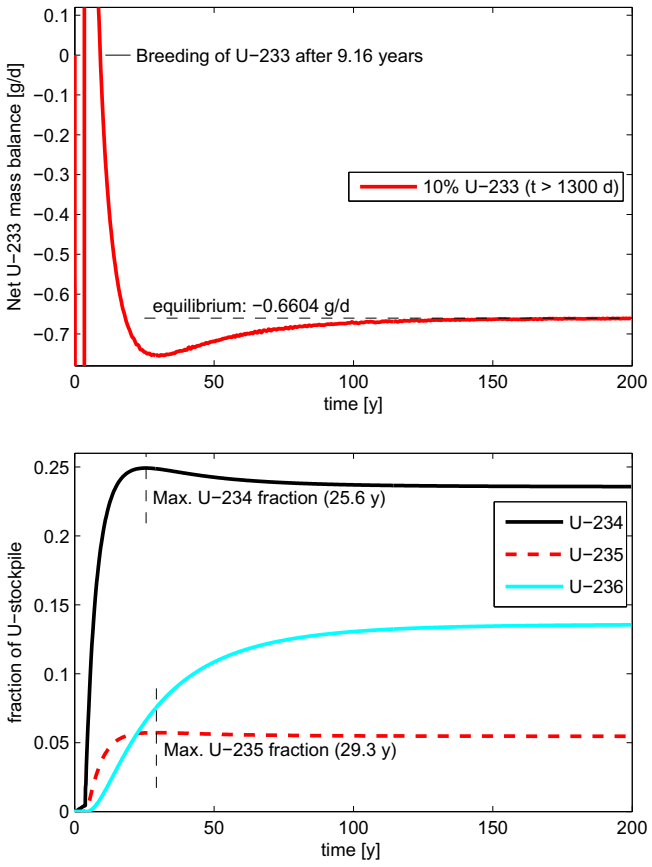

Fig. 5. Net U-233 mass flow balance of the system (top) and U-234, U-235 and U-236 fraction in the uranium stockpile (bottom) over time. The U-233 fueled phase is started after 1300 days. A 13% enrichment was used during the U-235 fueled phase.

These initial studies have given a good insight in some of the characteristics and time-scales of the running-in phase. There is still a shortage of reactivity in the initial stage of the U-235 fueled phase. Obviously, a higher enrichment of the driver fuel fed to the core is required in this initial stage to raise k_{eff} above unity. However, the enrichment should also be adjusted in a clever way to avoid large amounts of excess reactivity. Such studies can be performed, without analyzing the U-233 fueled phase. After choosing a proper strategy for the U-235 fueled phase, the U-233 fueled phase will be analyzed in order to reduce the excess reactivity during the U-233 fueled phase. Probably, this can help to achieve a net U-233 production at an earlier time. So, the following studies will be split up in an analysis of the U-235 fueled phase, followed by analyzing the U-233 fueled phase.

5.2. Flattening k_{eff} in the U-235 fueled phase

The k_{eff} changes quite a bit during the initial stage of the U-235 fueled phase. On the one hand, k_{eff} should be at least unity during the whole U-235 fueled phase, but one would also like to limit the maximum excess reactivity, for instance to 1%, to improve the fuel economy. Obviously, as Fig. 3a shows, this is not possible using a constant feed fuel enrichment. Therefore, a time dependent adjustment scheme for the feed fuel enrichment is studied in this section to limit the excess reactivity during the U-235 fueled phase.

Different strategies can be considered to adjust the U-235 feed rate, η_{U5}, during the U-235 fueled phase. A relatively simple scheme is chosen for the following studies and is given by

$$\eta_{U5}^{i+1} = \eta_{U5}^{i} - \alpha \frac{\left(k_{eff}^{i} - k_{eff}^{i-1}\right)}{\Delta t} - \beta\left(k_{eff}^{i} - k_{eff}^{desired}\right). \quad (17)$$

So, the U-235 feed rate of the new time-step η_{U5}^{i+1} is determined by adding two terms to the feed rate of the previous time-step η_{U5}^{i}. The first term is a proportionality constant α multiplied with the rate of change of k_{eff} and this term should stabilize k_{eff} on the shorter term. The constant α should be sufficiently large to ensure that rapid changes of k_{eff} can be sufficiently compensated by the feed fuel to ensure $k_{eff} > 1$. But a too large value of α will make the system unstable, because changing the feed fuel enrichment affects the reactivity over a long time-scale, i.e. proportional to the total driver pebble residence time.

The second term is a constant β multiplied by the difference between the actual k_{eff}^{i} and a desired final value: $k_{eff}^{desired}$. This term should ensure that the feed fuel enrichment is chosen in such a way that k_{eff} converges to the desired value of k_{eff} in the later stage of the U-235 fueled phase. The value of $k_{eff}^{desired}$ will be slightly larger than unity, e.g. 1.0002, to ensure the system is critical during any stage of the U-235 fueled phase.

Many other schemes may be considered to flatten k_{eff} by adjusting the feed fuel enrichment during the running-in phase. The advantage of this scheme is that it is rather simple and easy to implement. On the other hand, a disadvantage of this method is that the optimal values for α and β may differ among different reactor designs (and fuel management parameters). An interesting suggestion to resolve the latter problem would be an alternative scheme where the derivative of k_{eff} is minimized by adjusting the feed fuel enrichment within a first-order perturbation theory formulation. However, such a scheme is more cumbersome to implement and computationally more intensive due to the calculation of the adjoint fluxes, while the simple scheme of Eq. (17) will already prove to be quite effective for the current application.

5.2.1. Results

In the following, results will be shown for the U-235 fueled phase, using different values for α and β. Two goals should be achieved during the U-235 fueled phase. First, the k_{eff} should be above 1 during any stage of the running-in phase and preferably lower than 1.01, the latter value is in conjunction with the excess reactivity considered for the control rod positioning problem in previous work (Wols et al., 2014c). Secondly, one would like the k_{eff} to stabilize quickly around the value of $k_{eff}^{desired}$.

Fig. 6 shows k_{eff} as a function of time using different values of $\alpha/\Delta t$ (*top plot*) and β (*bottom plot*) to determine the enrichment of the feed fuel during the U-235 fueled phase. As the enrichment of the feed fuel is adjusted during each time-step in the calculation scheme, the flux shape is updated by DALTON at least every 20 Δt-steps during these calculations to ensure sufficient accuracy. The use of a larger coefficient $\alpha/\Delta t$ clearly reduces the maximum k_{eff}, but it takes longer to approach the desired k_{eff} of 1.0002. The use of a larger coefficient β can help to limit the maximum k_{eff} value and speed up approaching the desired k_{eff}. However, β should not be too high to avoid sub-criticality of the reactor and to avoid inducing oscillatory behavior of the k_{eff}.

A few other combinations of $\alpha/\Delta t$ and β have been investigated in Fig. 7. From the two graphs in Fig. 7, it can also be seen that the k_{eff} (*top*) responds very closely to changes in enrichment (*bottom*). Using a combination of a relatively strong coefficient $\alpha/\Delta t$ (=4.0) and β (=0.005) leads to a relatively fast approach of the desired k_{eff}, while the k_{eff} remains above unity for the whole U-235 fueled phase. Except for a few days of the initial stage ($k_{eff}^{max} = 1.0111$ after 9 days), the k_{eff} remains below 1.01 during the U-235 fueled phase.

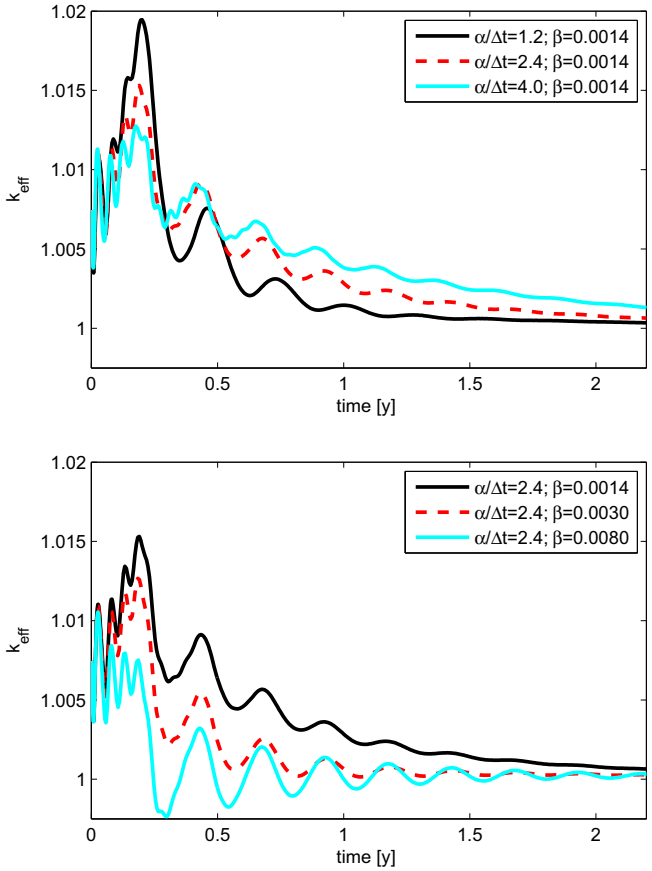

Fig. 6. k_{eff} as a function of time using different values of $\alpha/\Delta t$ (top) and β (bottom) to adjust the enrichment of the driver fuel, according to Eq. (17).

So, the enrichment over time prescribed by these coefficients is very suitable for the U-235 fueled phase.

However, the enrichment prescribed varies quite fast and quite a lot over time, i.e. between 11.9 w% and 16.3 w%. For practical application, it would be best to manufacture pebbles with a high enrichment, e.g. 17 w%, and pebbles with a low enrichment, e.g. 11 w% similar to the start-up core enrichment. To first order, the range of enrichments required during the U-235 fueled phase can then be attained by mixing of high enriched and lower enriched pebbles with the proper ratio. The difference in self shielding between a mixture with equal fractions of 11 w% and 17 w% enriched pebbles and the same amount of 14 w% pebbles is only a second order effect, which can also be compensated for by adjusting the fraction of higher enriched pebbles. Around 242 fresh driver fuel pebbles are added into the core per time-step of 2.5 h. So, even on such a short time-scale, a relatively fine regulation of the feed driver fuel enrichment is possible.

After the start of the U-233 fueled phase, a drop in the k_{eff} occurs, as can be observed in the Fig. 4a. In order to avoid k_{eff} from dropping below unity, an increase of the U-235 enrichment to 15% is used in the following calculations during the final 80 time-steps (8.33 days) of the U-235 fueled phase. Due to the increase of the enrichment, the k_{eff} increases from 1.0002 to 1.0085 at the start of the U-233 fueled phase.

5.3. Flattening k_{eff} in the U-233 fueled phase

The U-233 fueled phase is started after 1300 days, as this was shown to be the best option by the results in Fig. 4. For the first stage of the U-233 fueled phase, i.e. up to 25,000 time-steps or 7.13 years including the U-235 fueled phase, a similar scheme as in Eq. (17) is proposed to determine the U-233 weight fraction of the feed fuel. For a value of 4 for $\alpha/\Delta t$, the k_{eff} and the U-233 weight fraction of the feed driver fuel are shown as a function of time for β-values of 0.002, 0.003 and 0.004 in Fig. 8. A value of β of 0.005, like in the previous paragraph, led to k_{eff} values lower than unity. A value of β of 0.004 leads to a quick approach of the desired k_{eff} (of 1.0002), with little excess reactivity and without subcriticality.

Similar to the U-235 fueled phase, the flux shape profile was updated at least every 20 time-steps during the initial part of the U-233 fueled phase. Since a single five-group DALTON calculation takes around six minutes, a slightly different approach with larger flux update intervals, up to a maximum of 1000 time-steps per interval, should be chosen to avoid calculation times of several months for the remaining part of the U-233 fueled phase, up to 700,000 time-steps. It is also possible to lengthen the flux shape update interval, as Fig. 8 shows that k_{eff} is almost stable after 6 years, while the oscillations in the U-233 weight fraction have also damped out. There is still a slow increase of the U-233 weight fraction, associated with the long time-scale of saturation of the U-234, U-235 and U-236 fraction in the uranium stockpile, but this effect can also be described with a larger flux update interval. However, with a value of 4 for $\alpha/\Delta t$ and 0.004 for β, the scheme tends to become unstable and k_{eff} drops a bit below unity on such a longer flux update interval.

Different approaches are proposed to determine the U-233 weight fraction of the driver fuel during the remaining part of the U-233 fueled phase.

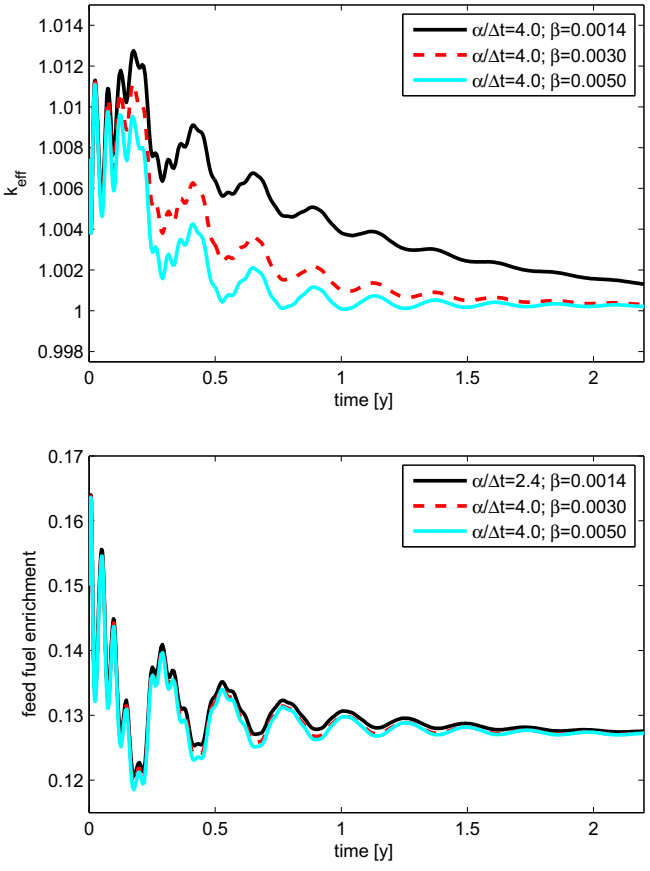

Fig. 7. The upper graph shows k_{eff} as a function of time using different values of $\alpha/\Delta t$ and β to adjust the enrichment of the driver fuel, according to Eq. (17). The lower graph shows the feed driver fuel enrichment as a function of time.

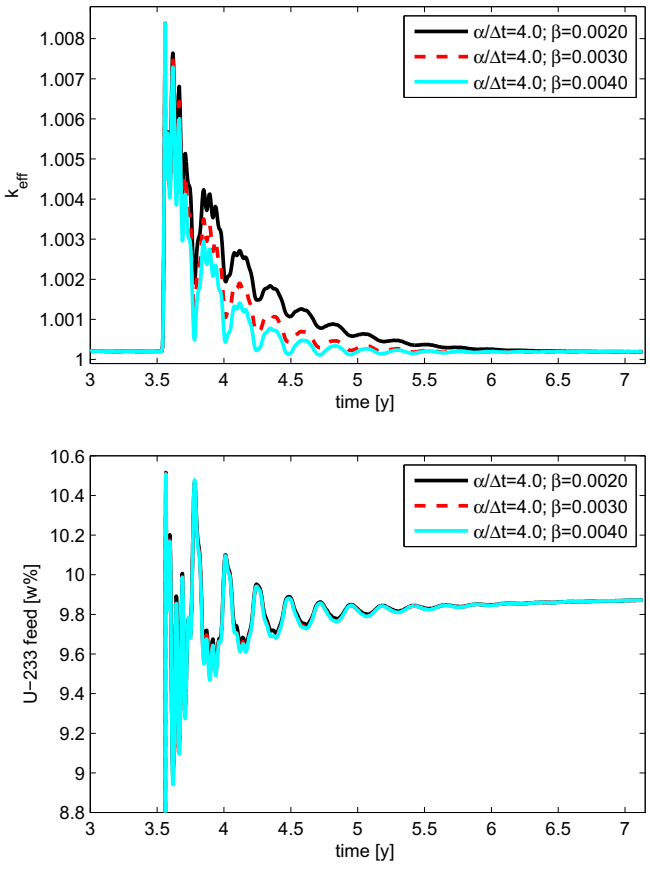

Fig. 8. The upper graph shows k_{eff} as a function of time for the initial part of the U-233 fueled phase, which starts after 1300 days, using different values of $\alpha/\Delta t$ and β to adjust the enrichment of the driver fuel, according to Eq. (17). The lower graph shows the U-233 weight fraction of the feed driver fuel as a function of time.

- Use a constant value of 10 w% U-233 in the fresh driver fuel pebbles after 25,000 time-steps. Only one pebble type will be required for the remaining part of the U-233 fueled phase, at the price of some additional excess reactivity. Ideally, one could even use 10 w% U-233 driver pebbles from the start of the U-233 fueled phase, so that only one fuel pebble type has to be manufactured, which would significantly ease fuel fabrication and lower production costs. However, this leads to a relatively high maximum k_{eff} of 1.0229. Results for both approaches will be shown in the following.
- Use Eq. (17), but with smaller coefficients $\alpha/\Delta t = 1.0$ and $\beta = 0.002$ to enhance stability. The changes of k_{eff} that have to be compensated are also much smaller and on a long time-scale in this part of the running-in phase, so smaller coefficients $\alpha/\Delta t$ and β should also suffice. The thresholds before doubling the length of the neutron flux update interval, as mentioned in Section 3.1.3, were increased to 10^{-7} for the flux shape change and 10^{-5} for the change of k_{eff}, to increase the stability of the calculation in combination with the U-233 weight fraction adjustment scheme.

The multiplication factor and the U-233 stockpile are shown as a function of time for these three approaches in Fig. 9. Clearly, the excess reactivity is rather large in case of using 10 w% U-233 driver fuel pebbles directly from the start of the U-233 fueled phase. Using a variable U-233 weight fraction for the fresh driver fuel pebbles limits the excess reactivity and criticality is approached rapidly. This also has a positive effect on the fuel economy of the system. The U-233 stockpile increases much quicker after breeding is achieved. Secondly, a net production of U-233 is already achieved after 6.3 years with a variable feed fuel U-233 weight fraction instead of after 9.3 years with a constant 10 w% U-233 weight fraction during the whole running-in phase. So, both in terms of limiting excess reactivity and improving the fuel economy, a variable U-233 weight fraction of the fresh driver fuel is preferred and this approach will also be used during the safety studies in the following section.

6. Passive safety during the running-in phase

In previous work (Wols et al., 2015), the 100 MW_{th} thorium breeder PBR was demonstrated to be passively safe within the equilibrium state. Obviously, one would also like such a reactor to operate in a passively safe manner during all stages of the running in phase. Therefore, a basic safety analysis is performed in this section. First, the impact of a DLOFC with scram is studied for various stages of the chosen running-in phase strategy, followed by a study of the uniform reactivity coefficient over time and a study of the maximum reactivity insertion due to water ingress.

DLOFC without scram scenarios were not simulated in this work. The temperature feedback of U-235/U-238 fuel is generally stronger negative than for Th/U-233 fuel, as will also be demonstrated in Section 6.2. Therefore, it can be anticipated that a failure to scram does not lead to a significant additional temperature increase during the initial part of the running-in phase, since the reactivity insertion by xenon decay can already be compensated

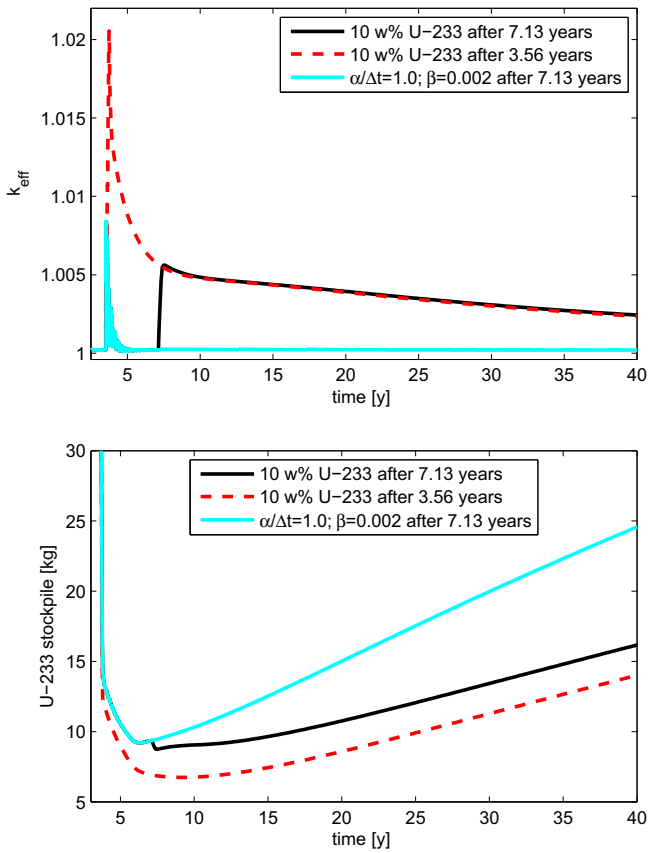

Fig. 9. k_{eff} as a function of time using three approaches for the U-233 fueled phase: A variable U-233 weight fraction is fed to the driver zone using $\alpha/\Delta t = 4.0$ and $\beta = 0.004$ until 7.13 years and 10 w% U-233 is used afterwards (case 1), or 10 w% U-233 is fed in the driver zone directly after 3.56 years (case 2) or a variable U-233 weight fraction with $\alpha/\Delta t = 4.0$ and $\beta = 0.004$ is used until 7.13 years and $\alpha/\Delta t = 1.0$ and $\beta = 0.002$ afterwards (case 3). The lower graph shows the U-233 stockpile as a function of time.

by a much smaller increase of the average core temperature. Furthermore, fully coupled transient simulations of a DLOFC without scram are very time-consuming to perform.

6.1. DLOFC with scram

A loss of pumping power and a depressurization of the core mark the beginning of a DLOFC transient, during which conduction and radiation are the main heat transfer mechanisms for decay heat removal. During the DLOFC transient, the maximum fuel temperature should remain below 1600 °C to ensure that radioactive fission products are retained within the coated fuel particles (Schenk et al., 1990). The maximum fuel temperature that occurs during a DLOFC with scram is strongly determined by the power density distribution over the core, especially the maximum power density, and the geometry of the core. Since the latter does not change over time, the change of the maximum power density (during normal operation) throughout the running-in phase is an important indication of how the maximum fuel temperature during a DLOFC with scram will be affected throughout the running-in phase, as compared to a DLOFC occurring in the equilibrium configuration. The evolution of the maximum power density (during normal operation) throughout the running-in phase is shown in the upper graphs of Fig. 10.

The maximum power density during normal operation fluctuates quite a bit during the initial part of the U-235 fueled phase. These fluctuations are a consequence of the variations in the enrichment of the feed driver fuel. The maximum power density quickly reaches a peak value of 8.74 MW/m^3. The fluctuations in maximum power density disappear after around a year, as the fluctuations in the feed fuel enrichment also decrease in magnitude, as shown in Fig. 7. During the remainder of the U-235 fueled phase, the maximum power density during normal operation slowly reduces as the U-233 concentration builds up in the breeder zone, resulting in a decrease of the fraction of the power produced in the driver zone. At the start of the U-233 fueled phase, some fluctuations in the maximum power density occur again due to the variation of the U-233 weight fraction in the fresh driver fuel during the initial part of the U-233 fueled phase. However, the maximum power density peak (7.45 MW/m^3) is smaller than in the U-235 fueled phase. Later on, the maximum power density slowly decreases to reach a value of 6.52 MW/m^3 after 10 years, 6.46 MW/m^3 after 40 years, and stabilizes at a value of 6.45 MW/m^3 after 200 years. This is slightly lower than the value of 6.89 MW/m^3 calculated with the more detailed equilibrium core model (Wols et al., 2015), including all relevant fission products and thermal–hydraulic feedback.

The maximum fuel temperature during a DLOFC with scram was also calculated for various stages of the running-in phase using the THERMIX code scheme. The geometrical THERMIX-model used is equivalent to the model used in previous work (Wols et al., 2015). The power density determined by DALTON in the running-in phase calculation scheme is used in a single THERMIX calculation to approximate the steady-state temperature distribution in the core, i.e. no thermal–hydraulic feedback is taken into account as the cross sections were generated for a single driver and breeder zone temperature. The steady-state temperature profile is used as the initial condition for the THERMIX calculation of the DLOFC with scram, which is calculated in a similar way as in the previous work (Wols et al., 2015). However, to save computation time, the transient calculation is performed without convection. This has only limited impact on the maximum fuel

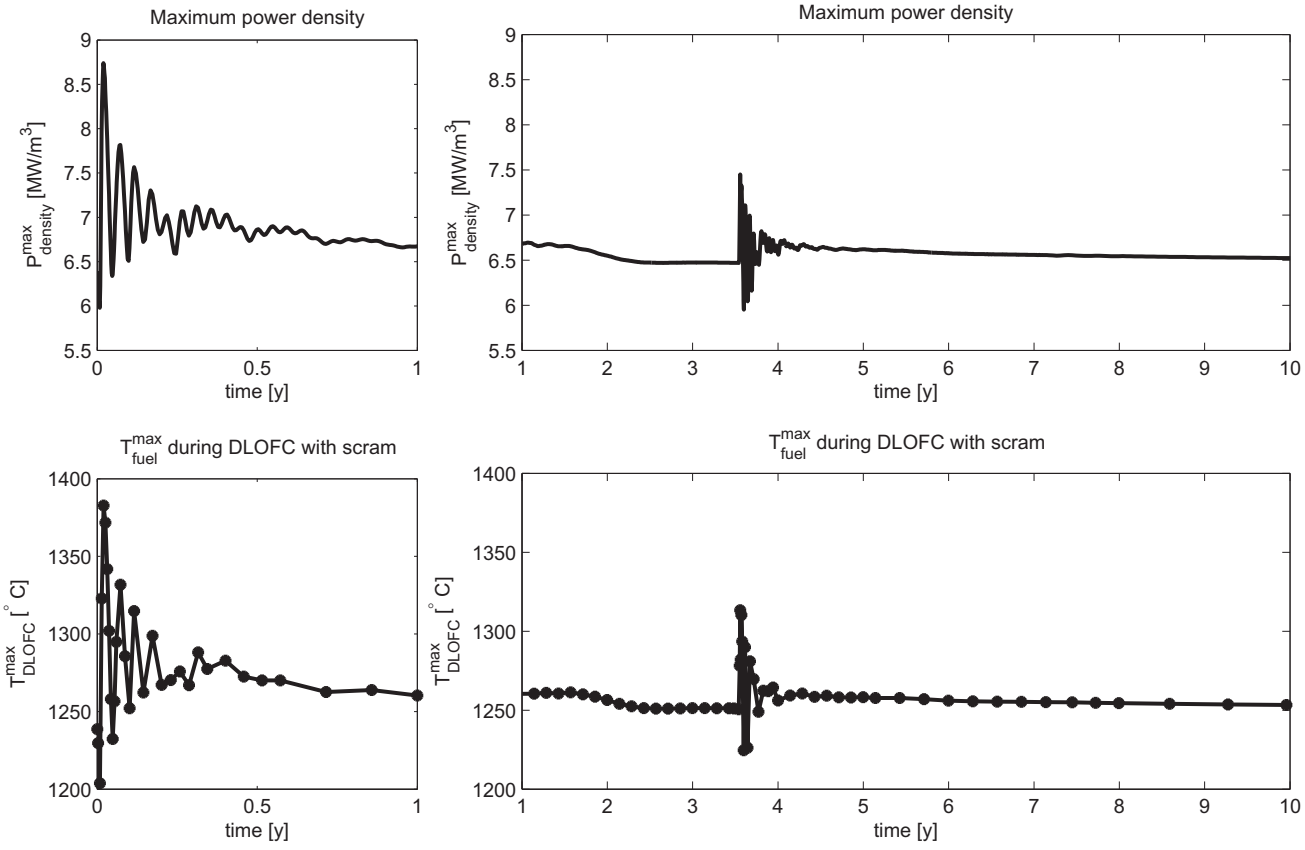

Fig. 10. Evolution of the maximum power density during normal operation throughout the running-in phase (top) and evolution of the maximum fuel temperature during a DLOFC with scram throughout the running-in phase (bottom). The U-233 fueled phase starts after 1300 days.

temperature, approximately +1 °C in comparison with a DLOFC calculation with convection, during the transient at atmospheric pressure and it is a conservative assumption, since the heat removal decreases slightly. The maximum fuel temperature during a DLOFC with scram is shown for various stages of the running-in phase in the lower graphs of Fig. 10.

The maximum fuel temperature after a DLOFC fluctuates quite a bit during the initial stages of the running-in phase, in a very similar manner as the maximum power density. Some small differences in these oscillations might be noticed because the maximum fuel temperature is simulated for less time-steps than the maximum power density. It reaches its maximum value (1383 °C) along with the maximum power density (8.74 MW/m^3). This maximum temperature is still quite a bit below the TRISO failure temperature of 1600 °C. At the start of the U-233 fueled phase, the maximum DLOFC temperature also fluctuates a bit, along with the U-233 weight fraction of the feed fuel and the maximum power density, but the peak temperature is much lower (1313 °C). At the end of the running-in phase, the maximum fuel temperature during a DLOFC with scram is 1250 °C, which is slightly lower than the value of 1280 °C calculated previously with the more detailed equilibrium core model (Wols et al., 2015). Such a difference could be expected due to the difference in the maximum power density, as discussed previously. Clearly, the maximum fuel temperature (+30 °C) predicted by the simplified scheme is not conservative for the equilibrium core, but the effect is fairly small compared to the remaining margin with respect to the TRISO failure temperature of 1600 °C.

6.2. Uniform reactivity coefficients and DLOFC without scram

The cross section generation methodology for the running-in phase model was explained in Section 3.2. In addition to the cross section set generated using the average equilibrium core temperature per radial zone, a similar cross section set was generated with a 500 K temperature increase. The uniform reactivity coefficient is determined by comparing the k_{eff}-values calculated by DALTON using these two cross section sets. The uniform temperature reactivity coefficient is shown as a function of time during the running-in phase in Fig. 11.

The reactivity coefficient is strongly negative (−11.2 pcm/K) for the start-up configuration with the uniform 11% enriched driver pebbles and rapidly weakens to a value of −8.2 pcm/K and then slowly becomes a bit stronger negative again. There is a rapid reduction of the reactivity coefficient's magnitude after starting the U-233 fueled phase (1300 days). Finally, a uniform reactivity coefficient of −3.68 pcm/K is achieved after 200 years. This value is very close to the value of −3.67 pcm/K calculated in previous work with a more detailed equilibrium core calculation model (Wols et al., 2015).

Since the reactivity coefficients are much stronger negative during the U-235 fueled phase, it can be expected that the reactivity insertion due to xenon decay during a DLOFC without scram can easily be compensated by the temperature feedback. Therefore, it can be expected that a DLOFC without scram leads to significantly lower maximum fuel temperatures after recriticality during the U-235 fueled phase than for the equilibrium core, which reaches a maximum temperature of 1481 °C during a DLOFC without scram due to the much weaker reactivity coefficient (Wols et al., 2015).

6.3. Water ingress

In view of passive safety, the reactivity insertion caused by water ingress should be compensated by a temperature increase of the core without the maximum fuel temperature exceeding 1600 °C to ensure the retention of radioactive fission products.

Cross section sets were generated using different levels of water ingress according to the cross section processing method discussed in Section 3.2, the water ingress itself was added into the cross section generation scheme in a similar way as in previous work by the authors (Wols et al., 2014b). For different stages of the running-in phase, the reactivity insertion due to water ingress was calculated for water densities ranging from 4 to 40 kg/m^3 of the total core volume (so helium plus pebble), increasing in steps of 4 kg/m^3. The maximum possible reactivity insertion over time is shown in Fig. 12.

During the U-235 fueled phase, the reactivity insertion due to water ingress first increases rapidly after uranium with a higher enrichment is fed to the core. It slowly decreases later on as the amount of fissile U-233 in the breeder zone slowly starts to increase, causing a lower requirement on the enrichment of the feed driver fuel to maintain criticality, which results in a less undermoderated state of the driver zone. In the final 80 time-steps of the U-235 fueled phase, the maximum reactivity insertion due to water ingress increases a bit due to the slight increase of the U-235 feed fuel enrichment. After the start of the U-233 fueled phase (1300 days), the maximum reactivity insertion due to water ingress strongly decreases as the U-233 replaces the U-235 in the

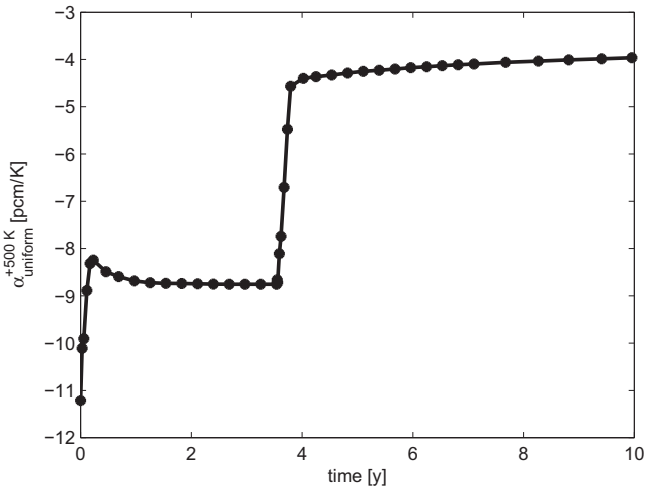

Fig. 11. Uniform temperature reactivity coefficient as a function of time during the running-in phase. These coefficients were calculated based on a uniform temperature increase of 500 K. The U-233 fueled phase starts after 1300 days.

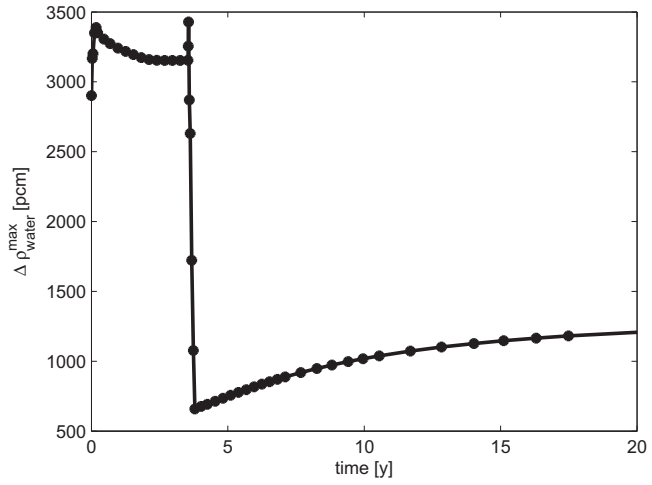

Fig. 12. Maximum reactivity insertion due to water ingress as a function of time during the running-in phase. The U-233 fueled phase starts after 1300 days.

driver zone. Afterwards, it slightly increases again and has a value of +1345 pcm after 200 years, when the equilibrium configuration is closely approximated. This value is a bit lower than the maximum reactivity insertion of +1497 pcm calculated in previous work by the authors (Wols et al., 2015), but this calculation also included a large number of fission products, actinides and thermal–hydraulic feedback to determine the steady-state power profile.

Water ingress can clearly cause a more severe reactivity insertion during the U-235 fueled phase, since the driver zone is in a stronger undermoderated state. However, even in absence of a reactor scram, this is not a real safety concern since the reactivity coefficient of the core is also much stronger negative in the U-235 fueled phase. So, also for the U-235 fueled phase, any reactivity insertion caused by ingress of water can eventually be compensated by the temperature feedback without exceeding the TRISO failure temperature of 1600 °C. It should also be noticed that the strong decrease of the uniform reactivity coefficient after the start of the U-233 fueled phase occurs simultaneously with the decrease of the maximum reactivity insertion due to water ingress. There is no transition moment where weak reactivity coefficients can lead to a dangerous temperature increase in case of water ingress.

The passive safety of the equilibrium core of the 100 MW_{th} thorium breeder PBR has been demonstrated previously by Wols et al. (2015). After investigating several safety parameters related to the severest incidents that can occur in a Pebble Bed Reactor, it can be concluded that the thorium breeder PBR can also fulfill the same passive safety requirements during the running-in phase.

7. Conclusions and recommendations

The studies presented in this work give an insight into the timescales involved in the running-in phase of a passively safe thorium breeder PBR. After using U-235/U-238 start-up fuel for 1300 days, the system starts to work as a breeder, i.e. the U-233 (and Pa-233) extraction rate exceeds the U-233 feed rate, within 7 years after start of reactor operation. Furthermore, the U-233 in the core at the end of reactor life can be used to start a new thorium PBR after reprocessing. So, the use of U-235/U-238 start-up fuel is only required for an extension of the fleet of thorium PBRs.

The studies also show that flattening the k_{eff} by a cleverly chosen time dependent scheme for the U-233 weight fraction or enrichment of the feed driver fuel, leads to a significant improvement of the fuel economy of the system and contributes to achieving breeding in a relatively short time (<7 years). Such a time dependent variation of the U-233 weight fraction can be realized in practice by manufacturing pebbles with two different enrichments, one enrichment lower than the lowest required and the other enrichment higher than the highest enrichment required, and inserting the pebbles into the core in ratios corresponding to the desired average time-dependent enrichment. The development of more practically applicable schemes to adjust the feed fuel enrichment or U-233 weight fraction over time, i.e. a scheme which describes the optimal enrichment to the operator for a certain state of the reactor, defined by a limited number of variables (or sensors), provides an interesting future research topic.

Furthermore, a basic safety analysis was performed for the chosen running-in phase strategy. Results show that passive safety is also ensured during the running-in phase. The maximum fuel temperature during a DLOFC with scram remains far below the TRISO failure temperature of 1600 °C (Schenk et al., 1990) during every stage of the running-in phase and the maximum temperatures are similar to a DLOFC occurring in the equilibrium core. Uniform reactivity coefficients are stronger negative for cores with U-235/U-238 driver fuel than in case of U-233/Th driver fuel. This ensures that water ingress, despite causing a stronger reactivity insertion for U-235/U-238 driver fuel, can be compensated by the temperature feedback. It should also ensure that the reactivity insertion due to xenon decay during a DLOFC without scram does not lead to a significant maximum fuel temperature increase in comparison with a DLOFC with scram during the initial stage of the running-in phase.

The calculations performed in the present work involved some simplifications. For improved accuracy of the results, it would be good to investigate the running-in phase using more radial depletion zones with a realistic radial pebble velocity profile. Though previous work (Wols et al., 2015) shows that the use of multiple radial depletion zones only has a limited impact upon the conversion ratio, it could somewhat delay the stabilization of the k_{eff} in the running-in phase (Marmier et al., 2013), as well as the desired fuel management strategy. Furthermore, including all fission products and relevant minor actinides into the depletion calculation should yield more accurate results and allows for studying the radiotoxicity of the nuclear waste. Finally, results of the DLOFC calculation could be somewhat improved by including the thermal–hydraulic feedback into the calculation of the steady-state power profile.

However, these modeling refinements are not expected to have a great effect on the trends observed in this work, i.e. the slow build-up of the U-234, U-235 and U-236 concentrations, the relevance of optimizing the fuel management strategy with respect to the fuel economy and the main observation that a net U-233 production can be achieved after a limited time within a passively safe thorium PBR.

References

Chang, H., Yang, Y., Jing, X., Xu, Y., 2006. Thorium-based fuel cycles in the modular high temperature reactor. Tsinghua Sci. Technol. 11, 731–738.

Marmier, A., Fütterer, M.A., Tucek, K., Kuijper, J.C., Oppe, J., Petrov, B., Jonnet, J., Kloosterman, J.L., Boer, B., 2013. Fuel cycle investigation for wallpaper-type HTR fuel. Nucl. Technol. 181, 317–330.

Massimo, L., 1976. Physics of High-Temperature Reactors. Pergamom Press.

Mulder, E., Serfontein, D., van der Merwe, W., Teuchert, E., 2010. Thorium and uranium fuel cycle symbiosis in a pebble bed high temperature reactor. In: High temperature Reactor Conference 2012, Prague, Czech Republic.

Oppe, J., Kuijper, J.C., de Haas, J.B.M., Verkerk, E.C., Klippel, H.T., 2001. Modeling of continuous reload HTR systems by the PANTHERMIX code system. In: M&C 2001, Salt Lake City, Utah, USA.

ORNL, 2009. SCALE: A Modular Code System for Performing Standardized Computer Analyses for Licensing Evaluations, vols. I–III, Version 6, CCC-750; ORNL/TM-2005/39. Radiation Safety Information Computational Center, Oak Ridge National Laboratory.

Rütten, H., Haas, K., 2000. Research on the incineration of plutonium in a modular HTR using thorium-based fuel. Nucl. Eng. Des. 195, 353–360.

Rütten, H., Haas, K.A., Brockmann, H., Ohlig, U., Pohl, C., Scherer, W., 2010. V.S.O.P. 99/09: Computer Code System for Reactor Physics and Fuel Cycle Simulation; Version 2009. Forschungszentrum Jülich.

Schenk, W., Pott, G., Nabielek, H., 1990. Fuel accident performance testing for small HTRs. J. Nucl. Mater. 171, 19–30.

Wols, F.J., Kloosterman, J.L., Lathouwers, D., van der Hagen, T.H.J.J., 2014a. Core design and fuel management studies of a thorium-breeder pebble bed high-temperature reactor. Nucl. Technol. 186, 1–16.

Wols, F.J., Kloosterman, J.L., Lathouwers, D., van der Hagen, T.H.J.J., 2014b. Preliminary safety analysis of a thorium breeder pebble bed reactor. In: PHYSOR 2014, Kyoto, Japan.

Wols, F.J., Kloosterman, J.L., Lathouwers, D., van der Hagen, T.H.J.J., 2014c. Reactivity control system of a passively safe thorium breeder pebble bed reactor. Nucl. Eng. Des. 280, 598–607.

Wols, F.J., Kloosterman, J.L., Lathouwers, D., van der Hagen, T.H.J.J., 2015. Conceptual design of a passively safe thorium breeder pebble bed reactor. Ann. Nucl. Energy 75, 542–558.

Xia, B., Li, F., Wu, Z., 2011. The simulation of the running-in phase of the HTR-10. In: ICONE-19. The 19th International Conference On Nuclear Engineering, Osaka, Japan.

Zheng, Y., Shi, L., 2008. Characteristics of the 250 MW pebble-bed modular high temperature gas-cooled reactor in depressurized loss of coolant accidents. In: High Temperature Reactor Conference 2008, Washington, DC, USA. HTR2008-58299.

Zheng, Y., Shi, L., Dong, Y., 2009. Thermohydraulic transient studies of the Chinese 200MWe HTR-PM for loss of forced cooling accidents. Ann. Nucl. Energy 36, 742–751.